A Family of Acoustic Vorticity Meters to Measure Ocean Boundary Layer Shear

Fredrik T. Thwaites, Albert J. Williams 3rd, Eugene A. Terray, and John H. Trowbridge.
Woods Hole Oceanographic Institution
Woods Hole, Ma. 02543

Abstract

We have developed several three axis acoustic vorticity meters at the Woods Hole Oceanographic Institution for measuring shear and turbulence in ocean boundary layers. Such a measurement, in principle, filters out irrotational motion such as linear surface gravity waves which can swamp measurements of a flow's rotational motion. We have constructed one 15 cm acoustic path instrument, four 45 cm path instruments, and one 1.5 m path instrument and established their accuracy in a series of laboratory and ocean experiments. The 15 cm acoustic path instrument has a mean flow induced vorticity error of 0.034 /s in a flow of 0.369 m/s and 20 dB rejection of waves. The 45 cm path instruments have an uncalibratable 10^{-2} /s mean flow induced vorticity error in a constant flow of 0.7 m/s consistent with the theoretical prediction that accuracy improves with increased path length. The 45 cm path instruments have been deployed in the ocean upper boundary layer to measure shear, in the thermocline to measure internal waves, and in the bottom boundary layer to measure turbulence.

I. INTRODUCTION

Oceanic boundary layer turbulence and mixing are driven in large part by vertical current shear. Measurements of turbulence or shear in the ocean boundary layers are difficult because turbulent and shear velocities are often swamped by currents and surface gravity waves. In any measurement of shear, vorticity or turbulence in the open ocean, one is trying to measure a small difference in the presence of large flow velocities. Typical ocean boundary layer velocities are of order 50 centimeters per second while shear is of order 0.01 per second. In measuring spatial differences there is usually a tradeoff between resolution and accuracy. To resolve this shear over 0.5 meters with current meters would require their accuracy to be better than 0.5 %. In the bottom boundary layer, measurement of turbulence near the sea floor in the coastal ocean is also difficult where wave-induced velocities can be orders of magnitude more energetic than turbulent velocities and occupy approximately the same frequency band.

This work was supported by the Office of Naval Research on grant N00014-94-1-0436 and the National Science Foundation under OCE-9018623. WHOI contribution number 8865 .

In the upper boundary layer comparison of shear to wind stress measures the effectiveness of vertical mixing in the boundary layer. This has importance for models of mixed layer deepening, heat transfer, and gas transfer in the presence of wave breaking and in the presence of organized of motions such as Langmuir cells. An additional problem in the upper boundary layer is wave bias that effects current and shear measurements made from current meters mounted on buoys or moorings that move with the waves [1]. The wave bias apparent shear can be as large or larger than the true Eulerian shear.

A nonintrusive measurement of vorticity would be immune to linear surface gravity waves, currents and wave bias. In order to address these difficulties, a family of vorticity sensors has been developed at the Woods Hole Oceanographic Institution.

II. DESIGN

In this family of vorticity sensors, circulation around a closed square path is measured which (via Stokes theorem) is the area-integrated vorticity over the surrounded area. A square was chosen for the circulation path to minimize apparent circulation in a constant mean flow. A triangle has fewer paths, but as Fig. 1 shows, a mean current could produce a wake on one side that would give a significant measured circulation where one did not exist in the undisturbed flow. The wakes resulting from a symmetrical square of transducers largely cancel out minimizing the vorticity error due to wakes.

The water velocity in each path around the square is measured acoustically. Differential acoustic travel times on each path are measured by modified Benthic Acoustic Stress Sensor (BASS) electronics [2]. The velocity of each path around the square is added (Fig 2) to give the circulation divided by the path length. In this paper, path length refers to a single acoustic path which makes up one side of a square. Circulation divided by path length is plotted instead of true circulation or vorticity because it has the same units as velocity so that cancellation of antiparallel velocities can be evaluated. The lab vorticity meter which will be described later, when oriented with two of the acoustic paths parallel to the flow, measures ten percent less velocity than the undisturbed flow. But the parallel paths have the same

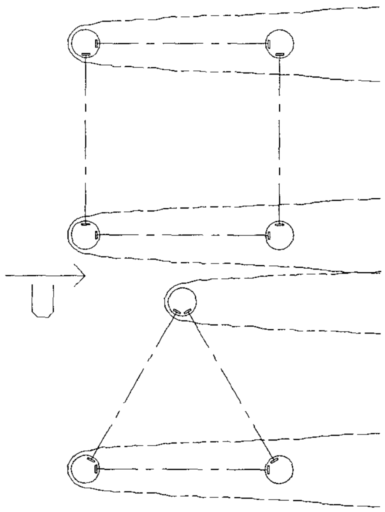

Fig. 1. Circulation error from transducer wakes cancel out with a square geometry but not with a triangle.

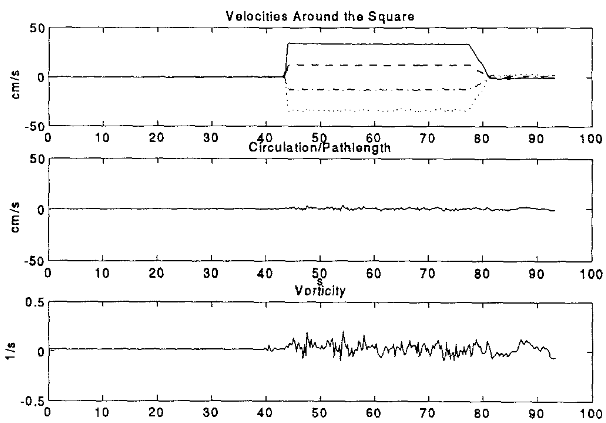

Fig. 2. Typical tow tank run showing measured velocity from each acoustic path around the square, circulation divided by path length, and vorticity. This sensor was at an angle to the flow.

decrement to within one percent, resulting in small vorticity error.

A three axis vorticity sensor was designed that minimized wake related errors. For an ocean buoy deployed instrument, all three axes of vorticity have to be measured because buoy attitude can change. Buoy motion can then be compensated in processing if the buoy's motion is known. A 15 centimeter acoustic path laboratory vorticity meter was made and is shown in Fig. 3. Twelve acoustic paths are the edges of a regular octahedron and form three orthogonal squares. Each sphere contains four piezoelectric transducers that form the corner of two circulation path squares. Since a flow sensor mounted on a buoy may see flow in any direction, and cannot be streamlined in all directions, the design philosophy was to minimize wake asymmetries and errors in circulation. This geometry maximized symmetry and minimized measured circulation flow disturbance. This prototype sensor was tested for bias in uniform flow in tow tanks and wave rejection in a wave tank and the results of these tests justified building several larger versions.

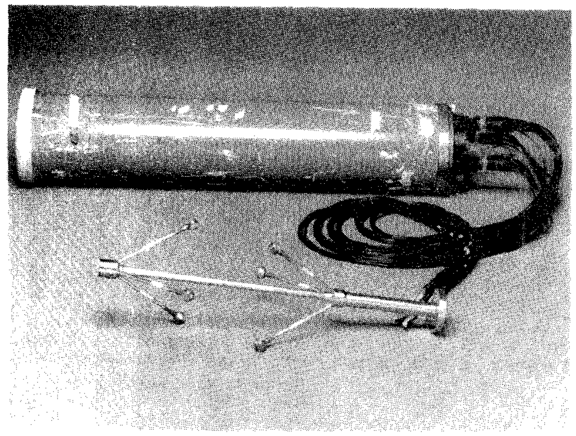

Fig. 3. Photo of the 15 cm acoustic path prototype three axis vorticity meter.

Circulation signal to wake induced noise is expected to increase with longer path length so the later instruments were scaled up from the prototype. Two 45 centimeter path length vorticity sensors were built into an inertially instrumented buoy to measure shear (Fig. 4). Two additional 45 centimeter path length vorticity sensors were built into a tripod and a 1.5 meter path length sensor was configured as its own tripod for measuring bottom boundary layer vorticity and shear [3].

The shear measuring buoy has a strapdown inertial measurement unit to measure buoy motion and remove it from measured relative flow. A free floating buoy moves with the long period swell and reduces relative flow and consequent wakes, but this movement must be measured. The inertial measurement unit consists of a triaxial accelerometer (Columbia model SA-307 HPTX), three single axis rate gyros mounted orthogonally (Systron Donner QRS-11 angular rate sensors), and a three axis magnetometer (Develco model 9200C). Sampled at 6.67 Hz, these inertial sensors enable rotations of the platform referenced vorticity measurements into the inertial earth frame. The measurement volumes are centered at 0.83 m and 2.45 m below the water surface. The electronics package is mounted well below the measurement volumes to reduce flow disturbance. The total buoy height is 5.06 m.

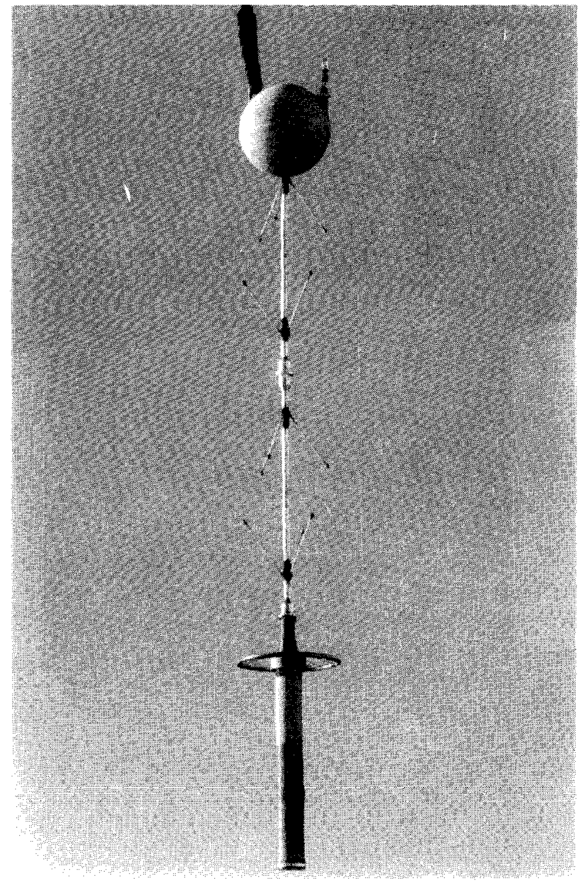

Fig. 4. Shear measuring buoy.

III. RESULTS

The first part of this section will describe a series of tests that established the vorticity meters' bias in constant flow, bias in a wave field, and spectral rejection of wave velocities. The rest of this section will describe two applications of the vorticity meters to measure shear in ocean boundary layers.

Both the 15 cm path length and 45 cm path length vorticity meters were drawn through tow tanks to establish their wake related vorticity error in uniform flow. As expected the larger sensor is more accurate. The 15 cm path vorticity meter measures a mean flow induced vorticity error of 0.034 /s in a flow of 0.37 m/s. This error is primarily from asymmetries between circulation paths and the wakes of the transducer spheres, sphere struts, and center tube. The electronic noise is well below wake related errors for velocities above a few cm/s. By increasing the acoustic path length while leaving the transducer spheres essentially the same size, the path integrated wake velocity defect (circulation error) stays the same. The area over which the vorticity is integrated increases as the square of the path length, thus greatly decreasing the vorticity error term. The center tube had to be scaled up proportionately with path length for structural reasons so its contribution to circulation error increased with path length. After dividing by path length squared (area) to get area average vorticity, this error goes as one over the path length. The vorticity error due to asymmetry in how the circulation path crosses the center tube wake can be calculated and removed in a constant flow. With the center tube wake error removed the 45 cm path vorticity meter measured a mean error of 0.01 /s in a 0.70 m/s tow. Removing this bias with the smaller sensor does not change the error significantly. Comparing the 15 cm and 45 cm sensor biases demonstrates the tradeoff between measurement volume (spatial resolution) and accuracy.

The vorticity bias in a wave field was estimated from an open ocean deployment of the shear measuring buoy, with significant swell and negligible wind stress. In a wave field with little or no mean relative current, the sensor's wake is advected back into the measurement volume, and the flow is accelerating in different directions, so constant flow accuracy results cannot be directly applied. Wake related errors will dominate all other errors in any open ocean condition and will scale with rms relative velocity. The buoy measured a mean horizontal vorticity of 0.0188 /s in an rms velocity wave field of 59 cm/s with an rms sensor relative velocity of 28 cm/s. For a conservative error estimate, it was assumed for this analysis that there was zero shear due to the low wind stress. This error is scaled with rms relative velocity in the error bars later in this paper.

The gradient Richardson number (1) is a ratio of the relative strengths of stratification, which inhibits mixing, and

$$Ri = \frac{N^2}{\left(\frac{dU}{dz}\right)^2} = \frac{-\frac{g}{\rho_o}\frac{d\rho_r}{dz}}{\left(\frac{dU}{dz}\right)^2} \qquad (1)$$

shear, which encourages mixing. N is the Brunt-Vaisala frequency, dU/dz is the vertical velocity shear, g is gravity, ρ_o is average density and $d\rho_r/dz$ is the density gradient. A gradient Richardson number less than one quarter is a necessary but not sufficient condition for turbulent vertical mixing to occur [4]. In the deployment described in the above paragraph, the measured local Brunt-Vaisala frequency was 0.011 /s (9.4 minute period). If the Richardson number was as low as 0.25 the shear could have been as large as 0.022 /s.

The 15 centimeter path sensor was tested in a wave tank to measure its spectral wave rejection and the results are shown in the frequency domain in Fig. 5. The sensor showed a rejection ratio of surface wave velocities of greater than 10. Most of the noise floor in Fig. 5 is residual turbulence in the tank from the waves and sensor wakes. The electronic noise floor in this measurement is about 1.8×10^{-4} cm^2/sec^2Hz. The longer path length vorticity sensors reject surface wave velocities by a greater ratio.

A bottom deployment of the 1.5 meter path vorticity sensor shows its spectral wave rejection. In May of 1994, the instrument was deployed near Woods Hole, Massachusetts in an area of Vineyard Sound having large tidal currents. The data shown in Fig 6 were measured during a storm with surface swell that reached the bottom. The measuring volume was centered 1.75 meters above the bottom. The power

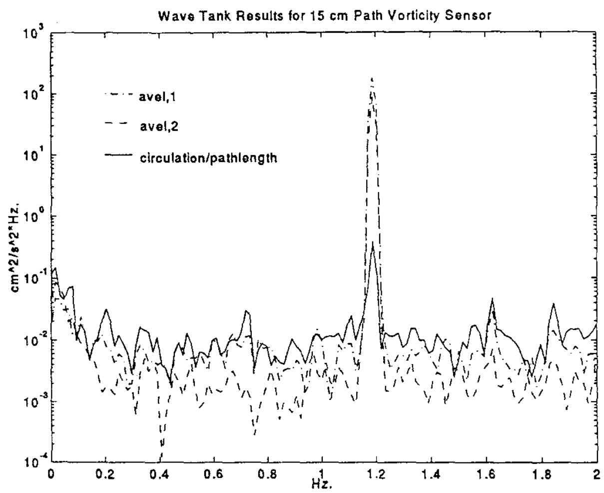

Fig. 5. Power spectral density of measurements in a wave tank.

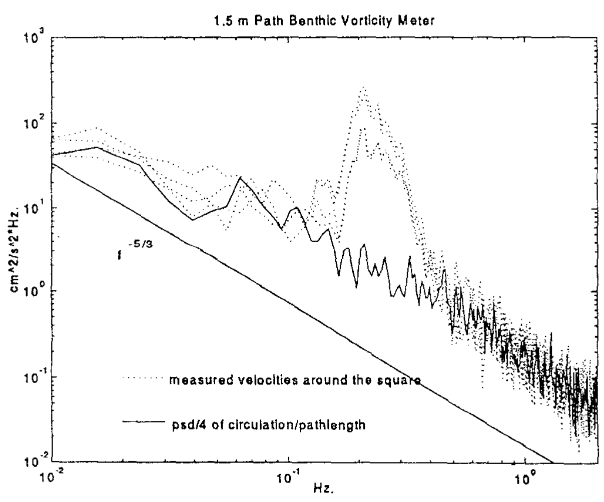

Fig. 6. 1.5 m benthic vorticity meter power spectral densities of acoustic path water velocities and circulation divided by path length.

spectral densities of the velocities of the individual acoustic paths making up a square are shown dotted and the power spectral density of circulation is shown solid. The power spectral density of circulation over path length has been scaled by one quarter to give the same energy at high frequencies as the velocity spectra. These data were reported in [3]. This instrument's effective surface wave rejection shows the utility of measuring vorticity.

The first application of the double 45 centimeter path shear measuring buoy to be discussed is measurement of shear in the upper ocean boundary layer. Shear, turbulence and mixing in unstratified turbulent boundary layers over rigid walls has been well studied and is well understood. By comparing the shear in an ocean boundary layer to the stress over this layer, the effect on mixing of the free surface, stratification, and possible organized motions like Langmuir circulation can be measured. The instrument was deployed in Buzzards Bay, Massachusetts in May of 1994. The wind stress was concurrently measured by a sonic anemometer and calculated using the inertial dissipation method [5]. The shear expected in the log layer next to a rigid wall is given by (2),

$$\frac{dU}{dz} = \frac{u_*}{\kappa z} \qquad (2)$$

where dU/dz is the shear, u_* is the friction velocity (the square root of the shear stress divided by density), κ is von Karman's constant usually assumed to be 0.4, and z the distance from the wall. The measured shears are compared to the shear one would expect in an unstratified rigid wall turbulent flow of the same shear stress (Fig. 7)[6]. The wind during the deployment increased in strength from about 5.2 m/s to about 15.2 m/s causing the water-side friction velocity to increase from 0.62 cm/s to 1.82 cm/s. The error bars are derived, as described above, from an open ocean deployment with significant swell and negligible wind stress and are scaled with rms velocity relative to the sensors. The shallower sensor at 0.83 meter depth, measured shear that coincided with the rigid wall turbulent shear prediction. The deeper sensor at 2.45 meter average depth, measured about 3 times more shear than would be predicted by a rigid unstratified wall layer. Average temperature stratification measured at this depth gave a Brunt-Vaisala frequency of 0.012 /s (period of about nine minutes), and the measured gradient Richardson number of the 2.45 m deep sensor, dropped from 0.20 to 0.10. These are reasonable Richardson numbers for a stressed boundary layer with turbulent mixing. The increased shear compared to the predicted shear of an unstratified boundary layer is a measurement of the stratification's inhibition of vertical turbulent mixing and consequent enhancement of shear.

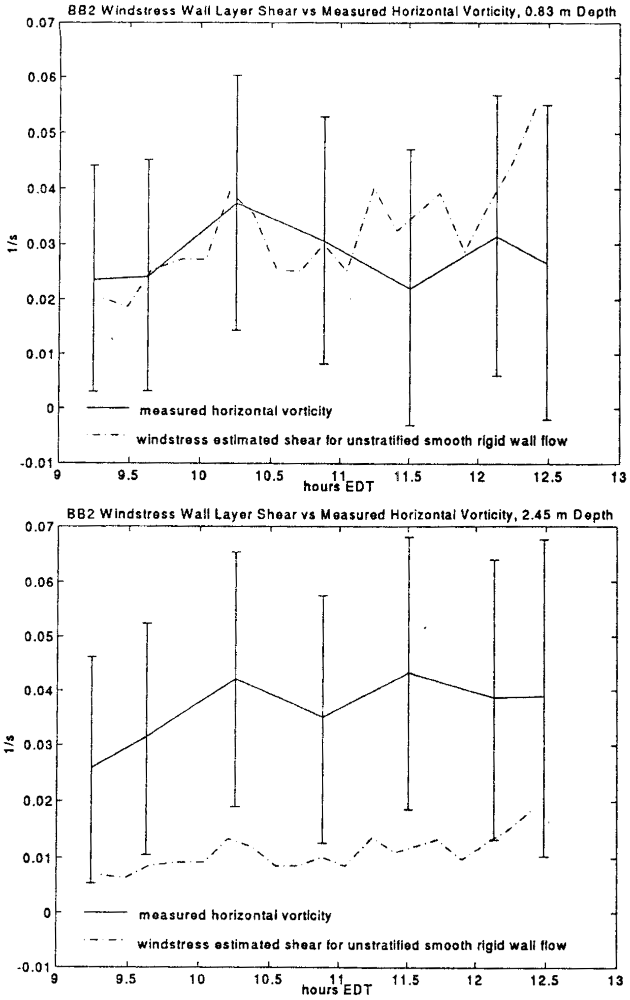

Fig. 7. Buzzards Bay deployment shears, measured and estimated from wind stress.

The second application to be discussed is measurement of shear and local shear instability in an internal boundary layer. In August of 1993 the shear measuring buoy was deployed with a single sensor in the thermocline in Massachusetts Bay. Fig. 8 shows a typical time history of temperature, magnitude of vertical shear, and gradient Richardson number. The histogram of gradient Richardson number is shown in Fig. 9. In this figure the histogram of Richardson number measured over a 1.0 meter bin size is also shown. The latter measurements were made the same day using an acoustic doppler current profiler (ADCP) to measure shear and CTD tow-yos to measure stratification. The 1.2Mhz ADCP averaging time was 30 seconds for this figure and the shear for both Figs 8 and 9 was lowpass filtered with a 25 second period filter. The greater proportion of low Richardson number measurements at the smaller vorticity meter 38.6 centimeter bin size than the ADCP 1.0 meter bin

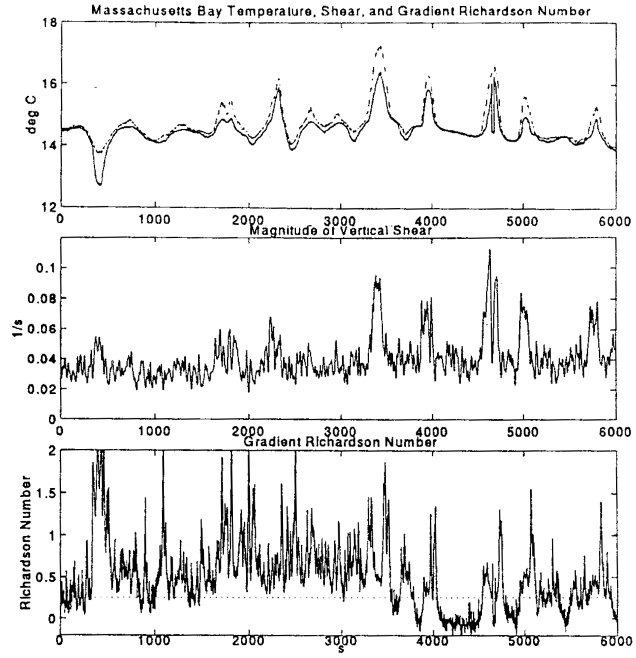

Fig. 8. Massachusetts Bay thermocline gradient Richardson number. In the top graph of temperature, the dot dash line is the temperature of the top of the measurement volume and the solid line is of the bottom. In Richardson number plot, a dotted reference line is drawn at 0.25.

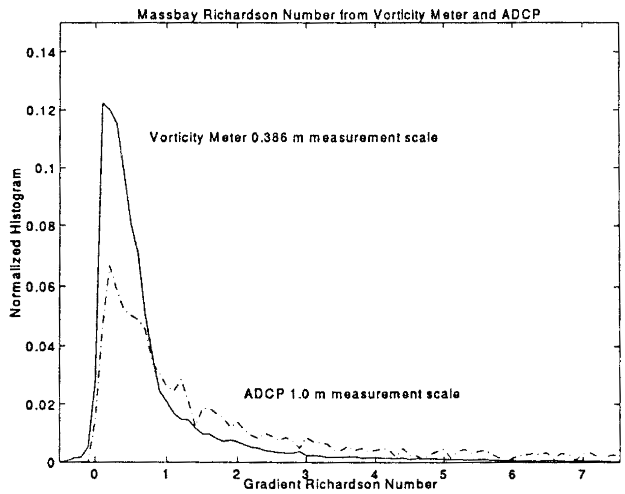

Fig. 9. Relative frequency of Richardson number measured over two length scales.

size is in agreement with the theory by Desaubies and Smith [7]. This deployment shows that this instrument can measure shear and local shear instability in ocean internal boundary layers.

IV. CONCLUSION

The family of three axis vorticity meters described here, has been shown to be a viable tool for measuring vertical shear in oceanic surface, internal and bottom boundary layers and turbulence in oceanic bottom boundary layers over small measurement volumes.

ACKNOWLEDGMENTS

Among the many people who have helped in this work are Jeff Hare who made the wind stress measurements during the Buzzards Bay deployment, Wayne Geyer who measured the ADCP gradient Richardson number in Massachusetts Bay and Gary Stanbrough who taught F.T.T. the art of potting transducers.

REFERENCES

[1] Pollard, R. "Interpretation of near-surface current meter observations," Deep-Sea Research, Vol. 20, 1973, pp. 261-268.

[2] Williams, A. J. III, J. S. Tochko, R. L. Koehler, W. D. Grant, T. F. Gross and C. V. R. Dunn "Measurement of Turbulence in the Oceanic Bottom Boundary Layer with and Acoustic Current Meter Array," Journal of Atmospheric and Oceanic Technology, Vol. 4, No. 2, 1987, pp. 312-327.

[3] Williams, A. J. III, E. A. Terray, F. T. Thwaites and J. H. Trowbridge "Acoustic Vorticity Meter for Benthic Boundary Layer Flow Measurements," Oceans 94, Vol III, pp. 250-253.

[4] Turner, J. S. *Buoyancy Effects in Fluids* Cambridge University Press, 1973, pp. 92-107.

[5] Fairall, C.W. and S.E. Larsen "Inertial Dissipation Methods and Turbulent Fluxes at the Air Ocean Interface," Boundary Layer Meteorology, 34, 1986, pp. 287-301.

[6] Monin, A. S. and A. M. Yaglom *Statistical Fluid Mechanics,* MIT Press, 1987, pp. 257-295.

[7] Desaubies, Y. and W. K. Smith "Statistics of Richardson Number and Instability in Oceanic Internal Waves" Journal of Physical Oceanography, Vol. 12, 1982, pp. 1245-1259.